CHEMISTRY
A EUROPEAN JOURNAL

FULL PAPER

DOI: 10.1002/chem.201302770

Probing DNA Mismatched and Bulged Structures by Using ^{19}F NMR Spectroscopy and Oligodeoxynucleotides with an ^{19}F-Labeled Nucleobase

Kazuhito Tanabe,* Takuya Tsuda, Takeo Ito, and Sei-ichi Nishimoto[a]

Abstract: In this study, DNA local structures with bulged bases and mismatched base pairs as well as ordinary full-matched base pairs by using ^{19}F NMR spectroscopy with ^{19}F-labeled oligodeoxynucleotides (ODNs) were monitored. The chemical shift change in the ^{19}F NMR spectra allowed discrimination of the DNA structures. Two types of ODNs possessing the bis(trifluoromethyl)benzene unit (F-unit) at specified uridines were prepared and hybridized with their complementary or noncomplementary strands to form matched, mismatched, or bulged duplexes. By using ODN F1, in which an F-unit was connected directly to a propargyl amine-substituted uridine, three local structures, that is, full-matched, G–U mismatch, and A-bulge could be analyzed, whereas other structures could not be discriminated. A molecular modeling study revealed that the F-unit in ODN F1 interacted little with the nucleobases and sugar backbone of the opposite strand because the linker length between the F-unit and the uridine base was too short. Therefore, the capacity of ODN F1 to discriminate the DNA local structures was limited. Thus, ODN F2 was designed to improve this system; aminobenzoic acid was inserted between the F-unit and uridine base so the F-unit could interact more closely with the opposite strand. Eventually, the G-bulge and T–U mismatch and the three aforementioned local structures could be discriminated by using ODN F2. In addition, the dissociation processes of these duplexes could be monitored concurrently by ^{19}F NMR spectroscopy.

Keywords: DNA · fluorine · molecular modeling · NMR spectroscopy · nucleobases

Introduction

DNA has programmable self-assembly features that facilitate the production of two- or three-dimensional structures, which are very important for the expression of the inherent functions of DNA in living organisms.[1–3] However, higher-order DNA structures are sometimes accompanied by the formation of incorrectly paired local structures, such as bulges and mismatches. The unpaired or bulged bases in double-stranded DNA are caused by insertions or deletions in replicated genes,[4–6] whereas the mismatched base pairs are a consequence of replication errors or heteroduplex formation during genetic recombination.[7–9] These irregular DNA structures are considered to play a major role in the production of proteins with incorrect sequences, which may lead to a nonfunctional gene product.[6] Thus, there are increasing demands for simple quantitative methods to facilitate the detection of higher-order DNA structures and local DNA structures that contain irregular base pairs and unpaired bases.

NMR spectroscopy is one of the best validated instruments for the quantitative analysis of chemical structures and conformations.[10–12] In particular, ^{19}F NMR spectroscopy provides distinct signals that facilitate the determination of molecular structures because of the high sensitivity of ^{19}F signals (approximately 83% of ^{1}H), the low concentration of endogenous ^{19}F atoms, and the lack of interference with ^{1}H signals.[13–15] Therefore, ^{19}F NMR spectroscopy has been used widely to obtain molecular information, even in complex biological conditions. Recently, several artificial oligonucleotides with ^{19}F-labeled substituents have been prepared to obtain valuable information regarding the conformations of DNA or RNA. ^{19}F-labeled nucleobases or ribose in oligonucleotides facilitate the monitoring of the formation of higher-order DNA or RNA structures,[16–23] DNA- or RNA–ligand interactions,[24–26] and RNA–protein interactions.[27]

^{19}F NMR spectroscopy and artificial oligonucleotides have been powerful tools for monitoring the global structures or extensive conformational changes, but conventional procedures have not been applied to detection of the specific local structures, such as bulges or mismatches, because the ^{19}F atoms in the oligonucleotides located too far from these irregular structures, which makes it difficult to discriminate them from normal structures. These research requirements prompted us to prepare appropriate ^{19}F-labeled oligonucleotides for monitoring mismatched and bulged DNA structures. We designed oligodeoxynucleotides (ODNs) where a bis(trifluoromethyl)benzene unit (F-unit) was introduced into a uridine ($d^{F1}U$ and $d^{F2}U$) through a rigid acetylene

[a] Dr. K. Tanabe, T. Tsuda, Dr. T. Ito, Prof. Dr. S.-i. Nishimoto
Department of Energy and Hydrocarbon Chemistry
Graduate School of Engineering, Kyoto University
Katsura Campus, Nishikyo-ku, Kyoto 615-8510 (Japan)
E-mail: tanabeka@scl.kyoto-u.ac.jp

Supporting information for this article is available on the WWW under http://dx.doi.org/10.1002/chem.201302770.

linker so that the NMR signal of the ^{19}F atom was susceptible to the DNA local structures and changes in the microenvironment around the F-unit. In this study, we prepared two types of ^{19}F-labeled ODNs (ODN F1 and ODN F2 shown in Figure 1). ODN F1, in which F-unit was connected directly

ODN F1 5'-ACG AGT ^{F1}UCG CAT-3'

ODN F2 5'-ACG AGT ^{F2}UCG CAT-3'

ODN 3 5'-ACG AGT TCG CAT-3'

ODN Comp 3'-TGC TCA AGC GTA-5'

ODN N-Bul 3'-TGC TCA$_{\llcorner N \lrcorner}$AGC GTA-5'

N = A, G, C, T

ODN G-Bul2 3'-TGC TCAA$_{\llcorner G \lrcorner}$GC GTA-5'

ODN N-Mis 3'-TGC TCA *N*GC GTA-5'

N = G, C, T

ODN ^{CF3}U 3'-TGC TCA ^{CF3}UGC GTA-5'

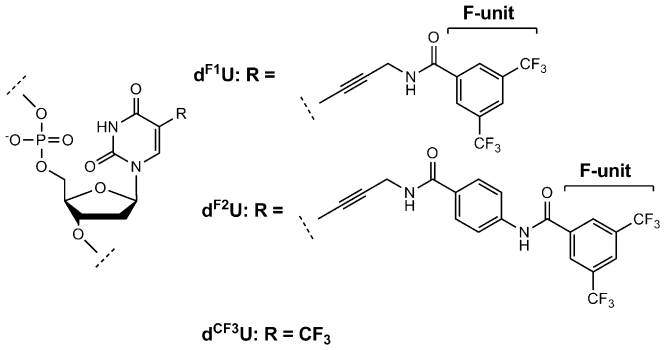

Figure 1. Sequences and chemical structures of oligodeoxynucleotides used in this study. Mismatched bases are shown in italic.

to a propargylamino group, could discriminate full-matched, G–^{F1}U mismatched, and A-bulged duplexes. We further designed ODN F2 to facilitate the highly sensitive detection of DNA local structures. To allow the F-unit to interact closely with irregular base pairs and the sugar backbone of the opposite strand, an aminobenzamido group was inserted between the F-unit and the propargylamino group to produce ODN F2. Ultimately, G-bulges and T–^{F2}U mismatches, and the three aforementioned local structures could be discriminated by using ^{19}F NMR spectroscopy with ODN F2, and the dissociation processes of these duplexes could also be monitored concurrently.

Results and Discussion

The synthetic route to artificial ODN F1 possessing d^{F1}U is shown in Scheme 1. An ODN possessing an amino group at a specified uridine base (ODN N) was prepared by automated DNA synthesis, as reported previously.[28] Coupling of *N*-hydroxysuccinimidyl ester **1** with ODN N gave the desired ODN F1.[29,30] The crude ODN F1 was purified by reversed

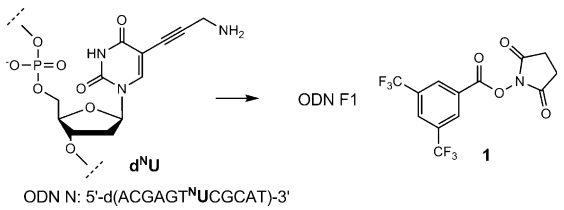

ODN N: 5'-d(ACGAGT^{N}UCGCAT)-3'

Scheme 1. Reagents and conditions: compound **1**, $NaHCO_3$, quant.

phase HPLC and the incorporation of d^{F1}U was confirmed by enzymatic digestion and ESI-TOF mass spectrometry.

ODN F1 was hybridized with its complementary DNA strand (ODN Comp) to form a duplex, and its stability was determined by monitoring the melting temperature (T_m) and measurement of circular dichroism (CD) spectrum in phosphate buffer (pH 7.0) containing 100 mM NaCl (Supporting Information, Figure S1). The ODN F1/ODN Comp duplex that contained a pair of d^{F1}U and A had a slightly lower T_m value by 2.6 °C than the reference duplex with an ordinary T–A pair (ODN 3/ODN Comp duplex). On the other hand, the CD spectrum of ODN F1/ODN Comp duplex showed a positive peak at 278 nm and negative peak at 254 nm. These results strongly indicate that the incorporation of d^{F1}U into the strand did not prevent duplex formation and that the global structure of the ODN F1/ODN Comp duplex was retained as a B-form as in the case of normal duplex consisted of ODN 3 and ODN Comp.

Initially, we monitored the duplex formation of ODN F1 and ODN Comp using ^{19}F NMR spectroscopy. As shown in Figure 2 A, the single-stranded ODN F1 showed a single signal at $\delta = -63.77$ ppm, whereas the addition of 0.33 equiv of ODN Comp to ODN F1 resulted in the appearance of a new signal at $\delta = -63.38$ ppm. Given that the ^{19}F signal of ODN F1 in duplex appeared as singlet, it is most likely that the rotation of the F-unit in the strand was not restricted, even in the duplex structure. The signal intensity at $\delta = -63.38$ ppm was increased by the further addition of ODN Comp up to 1 equiv of ODN F1, whereas the original signal of the single-stranded ODN F1 at $\delta = -63.77$ ppm disappeared almost completely. Since the signal change occurred as a function of the concentration of ODN Comp, we identified that the signal at $\delta = -63.38$ ppm was attributed to the duplex of ODN F1 and ODN Comp.

We next compared the ^{19}F NMR spectra of ODN F1 in the presence of strands, which formed mismatched base pairs, or a single bulge in the center of the duplex. These duplexes also showed concentration-dependent signal changes and their signals differed from that of single-stranded ODN F1 (Table 1). Duplexes possessing T–^{F1}U mismatch, C–^{F1}U mismatch, T-bulge, C-bulge, or G-bulge produced a single signal, which was attributed to the corresponding duplex, and the signals had a similar chemical shift to the full-matched duplex (ODN F1/ODN Comp). However, it was noted that the duplexes with an A-bulge and G–^{F1}U mismatch yielded distinct signals, which were shifted downfield compared with the full-matched duplex. Therefore, we could

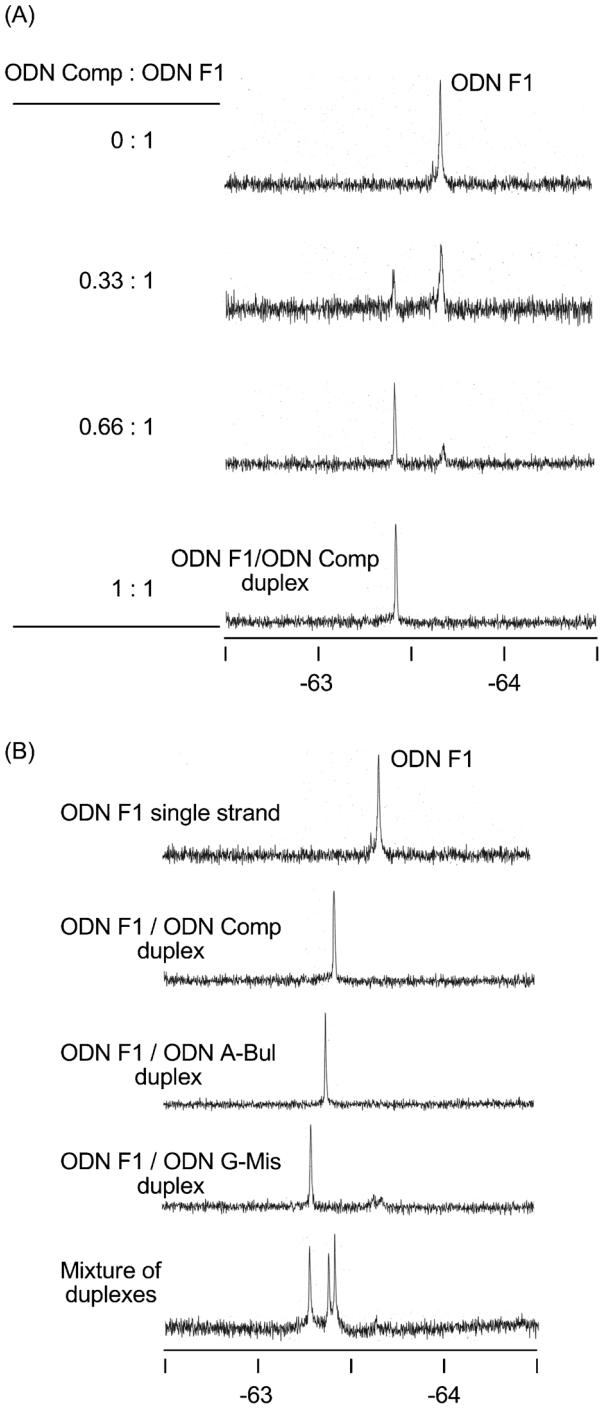

Figure 2. ^{19}F NMR spectra of ODN F1 in phosphate buffer (10 mM) containing NaCl (100 mM) at 26 °C. A) Duplex formation of ODN F1 (50 μM) in the presence of ODN Comp (0, 16.5, 33, and 50 μM); B) ^{19}F NMR spectra of each duplex (ODN F1/ODN Comp, ODN F1/ODN A-Bul, ODN F1/ODN G-Mis) and a mixture of these three duplexes as well as single-stranded ODN F1. The concentration of each duplex and single-stranded ODN F1 was 50 μM.

discriminate the formation of the full-matched duplex, G–^{F1}U mismatched duplex and A-bulged duplex using NMR spectroscopy even when these three duplexes were mixed in a single sample solution, as shown in Figure 2B.

Table 1. The chemical shift of the ^{19}F signal obtained from ODN F1 or ODN F2 in the presence of their complementary or noncomplementary strands.

Complementary or noncomplementary strands	ODN F1 δ [ppm]	ODN F2 δ [ppm]
–[a]	−63.77	−63.71
ODN Comp (full-match)	−63.38	−63.61
ODN A-Bul (A-Bulge)	−63.32	−63.55
ODN G-Bul (G-Bulge)	−63.38	−63.58
ODN C-Bul (C-Bulge)	−63.37	−63.60
ODN T-Bul (T-Bulge)	−63.37	−63.60
ODN G-Bul2	−63.35	–[b]
ODN G-Mis (G–U mismatch)	−63.20	−63.51
ODN C-Mis (C–U mismatch)	−63.38	−63.61
ODN T-Mis (T–U mismatch)	−63.37	−63.64

[a] Single-strand of ODN F1 or ODN F2. [b] No data.

Here, we will discuss the reason why the duplexes possessing G–^{F1}U mismatched, full-matched base pair or A-bulge gave discriminable ^{19}F signal. The chemical shifts suggest that F-units in mismatched duplexes possessing T–^{F1}U and C–^{F1}U pair and bulged duplexes possessing a C-, G-, and T-bulge were located in similar magnetic environment to that in the full-matched duplex to show a ^{19}F signal at similar chemical shift, whereas the F-unit in the duplexes possessing a G–^{F1}U mismatch and A-bulge were placed in different environments. It is well-known that a G base can form a hydrogen bond with a U base as well as a C base to form a wobble base pair.[31,32] Given that the melting temperature of ODN F1/ODN G-Mis duplex possessing a G–^{F1}U mismatch (T_m = 39.5 °C) was higher than that of other duplexes possessing a mismatched pair (C–^{F1}U mismatch: T_m = 31.2 °C, T–^{F1}U mismatch: T_m = 31.2 °C), the ^{F1}U base in ODN F1 probably formed a wobble base pair with G base in the ODN G-Mis. Thus, it is highly probable that the local structure around the G–^{F1}U mismatch was fixed by hydrogen bonding in a different way than the other duplexes did, thereby leading to the appearance of the ^{19}F signals of each F-unit at different chemical shifts. On the other hand, for the A-bulged structure, we assumed that the base sequence of ODN A-Bul was related to the change in the local structure, which caused the chemical shift differences. ODN F1/ODN A-Bul can form two types of A-bulged structures because ODN A-Bul has consecutive A bases that could form hydrogen bonds with ^{F1}U. One structure has an A-bulge at 5′-side of the A–^{F1}U base pair in the duplex, whereas the other has an A-bulge at the 3′-side of the A–^{F1}U base pair (Supporting Information, Figure S2). We speculated that ODN F1/ODN A-Bul formed a bulged structure at 5′-side of A–^{F1}U pair, unlike three other bulged duplexes possessing a G-, C-, and T-bulge, each of which formed a single bulge at the 3′-side of the A–^{F1}U pair. To investigate the correlation between the local structures of the bulged duplexes and their chemical shift changes, we prepared an ODN F1/ODN G-Bul2 duplex, which formed a G-bulge at 5′-side of A–^{F1}U pair, and we measured its NMR spectrum. A comparison of the ^{19}F NMR spectra revealed that the signal of ODN F1/ODN G-Bul2 could be discriminated from that of

ODN F1/ODN G-Bul (Table 1). Similar to the signal of the ODN F1/ODN A-Bul, the signal of the ODN F1/ODN G-Bul2 was shifted downfield, indicating that the formation of a bulged structure at 5′-side of the A–^{F1}U pair led to a downfield shift in the NMR spectrum to yield a distinct signal. Thus, the difference in the local structures of the A-bulged duplex consisted of ODN F1 and ODN A-Bul is most likely to cause the chemical shift change in NMR spectra.

As discussed above, we demonstrated that three duplexes possessing a full-matched base pair, a G–^{F1}U mismatch, and an A-bulge could be discriminated by using ^{19}F NMR spectroscopy with ODN F1. However, other duplexes gave signals with a similar chemical shift to the full-matched duplex, and thereby extensive discrimination of the bases in the strand and the local structures by NMR spectroscopy remains as a big issue to be solved. To verify the details of the molecular structure and to design a DNA probe with high performance, we conducted a molecular modeling study of the d^{F1}U-containing duplex. The structures of the d^{F1}U-containing duplexes were obtained from optimization of ODN F1/ODN Comp by using the AMBER* force field in water employing MacroModel. The F-unit was located in the major groove of the energy-minimized structures of the duplexes, probably because of its hydrophobicity (Supporting Information, Figure S3). As shown in Figure 3, molecular modeling of the duplex also revealed that the F-unit in ODN F1 was located approximately midway between two strands, because the linker that connected the F-unit and uridine base was too short (Figure 3A). Therefore, it seems that the close interaction between the F-unit and the nucleobase and sugar backbone on the opposite strand, which is critical for the discrimination of the local structures, was difficult. To discriminate further local structures on the opposite strand, we next designed ODN F2, which possessed a longer linker unit. Aminobenzoic acid was inserted between the F-unit and uridine, so the F-unit was closer to the opposite base and strand (Figure 3B). We expected that changes of base and the local structure would be discriminated with high sensitivity by ^{19}F NMR spectroscopic measurement of ODN F2.

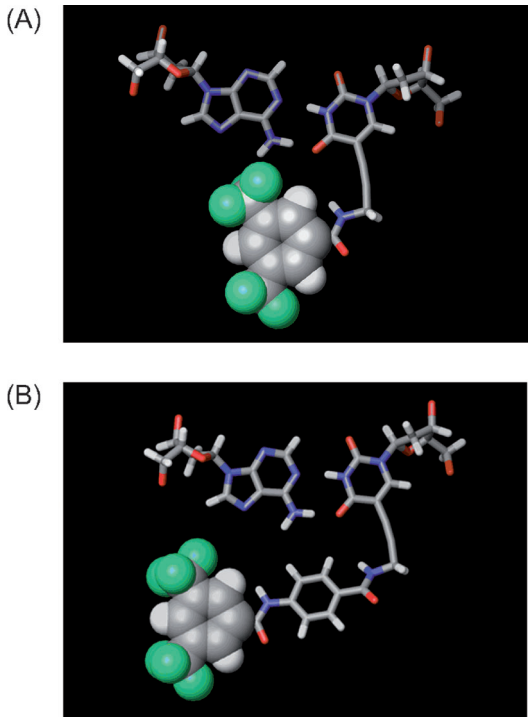

Figure 3. Molecular modeling of the simulated conformations of duplexes 5′-d(ACGAGTNCGCAT)-3′/5′-d(ATGCGAACTCGT)-3′ (N = ^{F1}U or ^{F2}U). The models were optimized by AMBER* force field in water by using the MacroModel version 9.1. The A) ^{F1}U–A, or B) ^{F2}U–A in the duplexes are highlighted. ^{19}F atom in F-unit is represented by green.

The synthesis of ODN F2 is illustrated in Scheme 2. Carboxylic acid **3**, which was synthesized from methyl *p*-aminobenzoate **2**, was coupled to *N*-hydroxysuccinimide to give **4**.

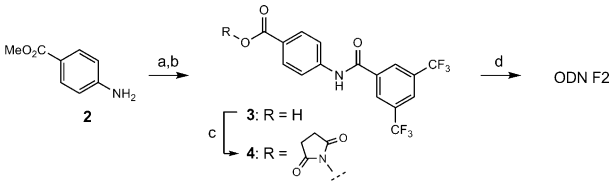

Scheme 2. Reagents and conditions: a) 3,5-bis(trifluoromethyl)benzoic acid, 1-hydroxybenzotriazole (HOBt), *N*′-(3-dimethylaminopropyl)-*N*-ethylcarbodiimide (EDC), 57%; b) NaOH, THF, MeOH, 86%; c) *N*-hydroxysuccinimide, EDC, HOBt, 47%; d) ODN N, $NaHCO_3$, quant.

ODN F2 was prepared by the coupling of **4** with ODN N. Measurements of T_m and the CD spectra of the ODN F2/ODN Comp duplex indicated that ODN F2 formed a stable B-type duplex with ODN Comp in a similar manner to ODN F1 (Supporting Information, Figure S1).

To gain further insights into the structures of duplexes consisting of ODN F1 and ODN F2, we measured their ^{19}F NMR spectra and differential NOE. As the opposite strand of ODN F1 and ODN F2, we prepared ODN ^{CF3}U, in which CF_3 group was incorporated into a specified uridine. The uridine modified by the CF_3 group (d^{CF3}U) was placed at the interior of the strand so as to be in close contact with the F-units in ODN F1 and ODN F2. Figure 4 shows the ^{19}F NMR spectra and ^{19}F–^{19}F differential NOE spectra of the ODN F1/ODN ^{CF3}U duplex and ODN F2/ODN ^{CF3}U duplex at 10 °C. The single signal of F-unit in the ODN F2/ODN ^{CF3}U duplex appeared at $\delta = -62.93$ ppm and we also observed a single signal from the CF_3 group in ODN ^{CF3}U at $\delta = -62.83$ ppm (Figure 4D). The F-unit in ODN F2 exhibited NOE related to CF_3 group in ODN ^{CF3}U (Figure 4C), indicating that ODN F2 and ODN ^{CF3}U formed a duplex with a single conformation, and the F-unit and CF_3 group in ODN ^{CF3}U were located in close proximity as designed. On the other hand, from ODN F1/ODN ^{CF3}U duplex, two signals at $\delta = -63.03$ and -63.09 ppm assigned to CF_3 group in ODN ^{CF3}U and a broad signal at $\delta = -62.70$ ppm assigned to F-unit in ODN F1 appeared, but no NOE was detected between these two groups (Figure 4A and B). The ODN F1/

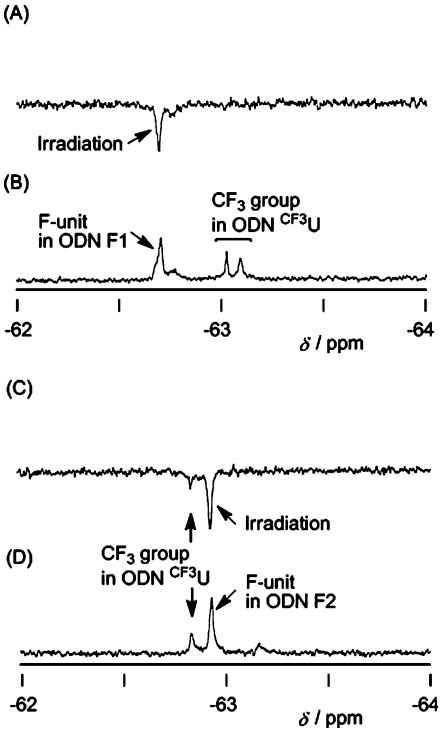

Figure 4. ^{19}F–^{19}F differential NOE spectra (A and C) and ^{19}F NMR spectra (B and D) of ODN F1 (A and B) or ODN F2 (C and D) in the presence of ODN ^{CF3}U. All spectra were measured in aqueous solution containing NaCl (100 mM), phosphate Na (50 mM, pH 7.0) and D_2O (20%) at 10 °C. A) Irradiation at $\delta = -62.70$ ppm (F-unit in ODN F1); B) basic spectrum of ODN F1/ODN ^{CF3}U duplex; C) irradiation at $\delta = -62.93$ ppm (F-unit in ODN F2); D) basic spectrum of the ODN F2/ODN ^{CF3}U duplex.

ODN ^{CF3}U duplex seems to form a duplex with several conformations, in which F-unit and CF_3 group in ODN ^{CF3}U were not close because of the short linker between the F-unit and its conjunct uridine in ODN F1.

We next compared the ^{19}F NMR spectra of ODN F2 in the presence of several strands with complementary or noncomplementary sequences. As shown in Figure 5A, ODN F2 could discriminate three structures including the G–^{F2}U mismatched base pair, the A-bulged structure, and the full-matched pair, similar to the case of ODN F1. It was striking that an additional G-bulged structure and a T–^{F2}U mismatched duplex yielded ^{19}F signals with different chemical shifts.[33] Therefore, we could discriminate five duplexes and single-stranded ODN F2 by using ^{19}F NMR spectroscopy. These results strongly suggest that the F-unit in ODN F2 interacts closely with the opposite strand, thereby facilitating the discrimination of bulged structures and mismatched duplexes. In light of the ^{19}F NMR spectroscopic properties of ODN F2, further attempts were made to monitor the dissociation of five pooled duplexes by using ^{19}F NMR spectroscopy. We prepared a mixture of these five duplexes and single-stranded ODN F2, and monitored the change in the ^{19}F NMR spectra as the temperature increased. At 26 °C, we observed six signals, which were attributed to duplexes with G–^{F2}U mismatched (i), A-bulged (ii), G-bulged (iii), full-matched (iv), and T–^{F2}U mismatched (v) structures, as well as single-stranded ODN F2 (vi) at $\delta = -63.51$, -63.55, -63.58, -63.61, -63.64, and -63.70 ppm, respectively (Figure 5B). When the measurement temperature was raised from 26 to 36 °C, the ^{19}F signals of (iii) and (v), which were attributed to G-bulged and T–^{F2}U mismatched structures, attenuated gradually and mostly disappeared at 42 °C. By contrast, the ^{19}F signal of (vi) with single-stranded ODN F2 became slightly intense (Supporting Information, Figure S4). These results strongly indicate that G-bulged and T–^{F2}U mismatched duplexes dissociated to form single strands as elevating the temperature. Further elevations of the temperature led to the disappearance of the ^{19}F signals of (i) and (ii), which were attributed to the G–^{F2}U mismatched and A-bulged duplexes. At 46 °C, these duplexes dissociated to form single strands, so only the two signals of the full-matched duplex (iv) and single-stranded ODN F2 (vi) remained. Eventually, the signal of the full-matched duplex disappeared at 56 °C, thereby resulting in the formation of single-stranded ODN F2. Thus, we could use ^{19}F NMR spectroscopy to monitor the simultaneous dissociation of several duplexes into single strands.

The NMR spectra of ODN F2 provided quantitative information related to the hybridization properties of these duplexes. We next assessed the T_m of these duplexes based on the signal intensity of each duplex. T_m was defined as the temperature at which half of the strands were in the duplex form or single-stranded state. Therefore, T_m was estimated as the temperature at which the intensity of the ^{19}F signal obtained from each duplex was reduced by half. As shown in Figure 6, the intensities of the ^{19}F signals of each duplex reduced with increasing temperatures, whereas those of single strands increased (Supporting Information, Figure S4). Based on the changes in the ^{19}F signal intensity, we calculated the T_m value for each duplex. As summarized in Figure 6B, the T_m values calculated from the ^{19}F signal intensity were exactly the same as those obtained from the UV measurement of duplexes individually, which is the conventional procedure used to estimate T_m values. Thus, we could monitor the dissociation of several duplexes concurrently and measure the T_m value by using ^{19}F NMR spectroscopy.

Conclusion

We have demonstrated a quantitative method to discriminate DNA local structures by using ^{19}F NMR spectra. We successfully prepared two types of ^{19}F-labeled ODNs and measured their ^{19}F NMR spectra in the presence of their complementary or noncomplementary strands. ODN F1, in which F-unit was linked to a uridine base through a propargylamino group, provided evident ^{19}F signals that corresponded to full-matched, A-bulged, and G–^{F1}U mismatched duplexes as well as single strand, and thereby we could discriminate these structures by one-dimensional ^{19}F NMR spectra. An improved DNA probe, ODN F2, in which the

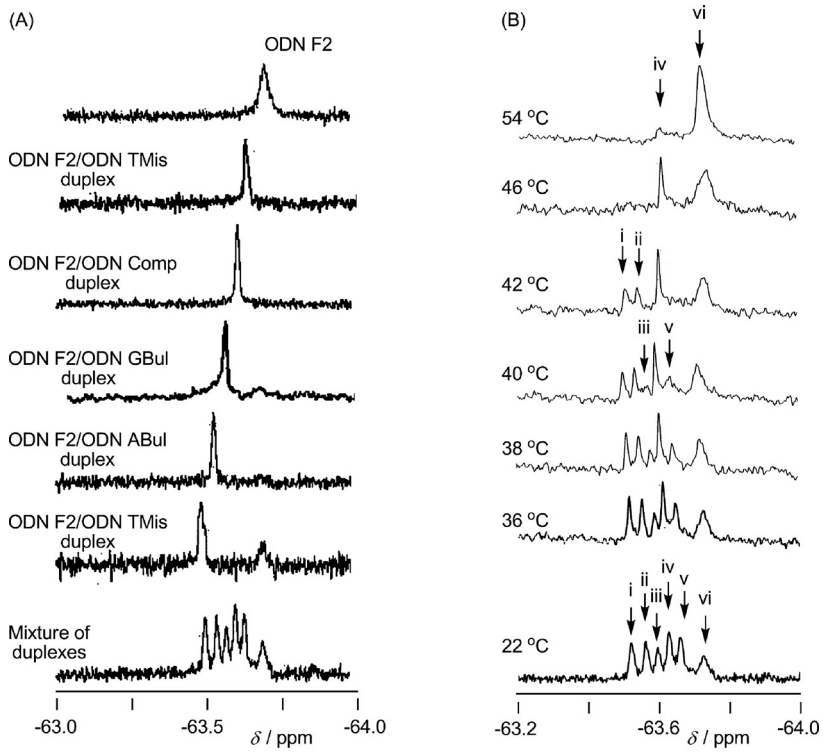

Figure 5. ^{19}F NMR spectra of ODN F2 in phosphate buffer (10 mM) containing NaCl (100 mM). A) ^{19}F NMR spectra of each duplex (ODN F2/ODN T-Mis, ODN F2/ODN Comp, ODN F2/ODN G-Bul, ODN F2/ODN A-Bul, ODN F2/ODN G-Mis) and a mixture of these five duplexes as well as single stranded ODN F2. All spectra were obtained at 26 °C. B) ^{19}F NMR spectra of the mixture of five duplexes and single-stranded ODN F2 measured at different temperatures. The signal of each duplex is indicated by roman numerals; i: ODN F2/ODN G-Mis duplex; ii: ODN F2/ODN A-Bul duplex; iii: ODN F2/ODN G-Bul duplex; iv: ODN F2/ODN Comp duplex; v: ODN F2/ODN T-Mis duplex; vi: single-stranded ODN F2. The concentration of each duplex and single-stranded ODN F2 was 50 μM.

F-unit and uridine were linked through a propargylamine–benzoic acid conjugate, also gave apparent signals for T–^{F2}U mismatched and G-bulged duplexes, as well as signals for the four structures described above. Molecular modeling of the simulated conformations of the duplexes revealed that the F-unit was located in the major groove of duplexes and the F-unit in ODN F2 could interact closely with the opposite strand to give a distinct signal corresponding to its target structure. The dissociations of mixed duplexes possessing several local structures could be monitored with increasing temperature, and therefore we could estimate the melting temperatures of each duplex concurrently. Thus, the behaviors of DNA duplexes were quantitatively monitored by the measurement of ^{19}F NMR spectra.

Experimental Section

General method: Reagents were purchased from Wako pure chemical industries, Nacalai tesque and Aldrich, Tokyo chemical industry, and Invitrogen and used without purification. The course of reactions was monitored by thin-layer chromatography (TLC) on fluorescent silica gel plates (Silica Gel 60 F254) by using UV light. Wakogel C-300 was used for silica gel chromatography. UV/Visible spectra were measured with a JASCO V-630 UV/Vis spectrophotometer. ODNs were synthesized with Applied Biosystems 3400 DNA Synthesizer. Synthesized ODNs were purified by reversed phase HPLC L-2000 series (Hitachi High-technologies) equipped with a Inertsil ODS-3 column (GL science Inc.). The solvent mixture of triethylamine acetate (TEAA; 0.1 M), pH 7.0, and 100% acetonitrile was delivered as the mobile phase at a flow rate of 0.6 or 3.0 mL min^{-1} at 40 °C. CD spectrum was measured with a J-805 spectropolarimeter. ESI-TOF mass spectrometry was measured with a Thermoscientific exactive. FAB mass spectra were measured with a JMS-SX102 A-(JEOL) mass spectrometer, using 3-nitro benzyl alcohol (NBA) as a matrix and polyethylene glycol (PEG 600) as an internal calibration standard. ^{1}H NMR spectra were measured with JEOL JNM-AL 300-(300 MHz) or JEOL EX-400-(400 MHz) spectrometer.^{1}H NMR spectra and C-coupling constants (J value) are reported in Hertz. The chemical shifts are expressed in ppm downfield from tetramethylsilane, using residual chloroform ($\delta=$ 7.24 ppm in the ^{1}H NMR spectra, $\delta=$ 77.36 ppm in the ^{13}C NMR spectra) as internal standards. Multiplicity is designed as singlet (s), doublet (d), triplet (t), quartet (q), or multiplet (m). ^{19}F NMR spectra were measured with JEOL EX-400(376 MHz) spectrophotometer at ambient temperature. Compound **1**[34] and ODN N[28] were synthesized as described previously. ODN ^{CF3}U was prepared by automated DNA synthesis using commercially available reagents. All aqueous solutions were prepared using purified water (YAMATO, WR600 A).

4-[3,5-Bis(trifluoromethyl)benzamido]benzoic acid (3): Methyl 4-aminobenzoate **2** (334 mg, 2.21 mmol), 3,5-(bistrifluoromethyl)benzoic acid (316 mg, 1.20 mmol), 1-hydroxybenzotriazole (HOBt; 288 mg,2.12 mmol), and *N*′-(3-dimethylaminopropyl)-*N*-ethylcarbodiimide (EDC; 394 mg, 2.53 mmol) were dissolved in dry DMF (8.0 mL) and stirred for 8 h at 80 °C. After diluting with water, the reaction mixture was extracted with ethyl acetate. The organic layer was washed by brine, dried over anhydrous $MgSO_4$, filtered and then concentrated in vacuo. The crude product was purified by flash chromatography (SiO_2, 0.25% methanol/chloroform) to give methyl 4-[3,5-bis(trifluoromethyl)benzamido]benzoate (491 mg, quant) as yellow solid. ^{1}H NMR (400 MHz, $CDCl_3$): $\delta=3.84$ (s, 3H), 7.93 (d, $J=8.8$ Hz, 2H), 8.00 (d, $J=8.76$ Hz, 2H), 8.39 (s, 1H), 8.60 ppm (s, 2H); ^{13}C NMR (75 MHz, $CDCl_3$): $\delta=52.16$, 119.68, 126.64, 127.56, 130.93, 131.59, 132.24, 132.69, 136.67, 141.40, 162.96, 166.47 ppm; FABMS (NBA): m/z: 392 $[M+H]^+$; HRMS calcd for $C_{17}H_{12}F_6NO_3$ 392.0721 $[M+H]^+$; found: 392.0718.

An aqueous solution of 5 M NaOH (1.0 mL) was added to a solution of methyl 4-[3,5-bis(trifluoromethyl)benzamido]benzoate (183 mg, 0.466 mmol) in methanol (5 mL) and THF (5 mL), and the resulting mixture was stirred for 20 h at 40 °C. After the reaction, the mixture was extracted by ethyl acetate. The organic layer was washed by brine, dried over anhydrous $MgSO_4$, filtered and then concentrated in vacuo to give crude **3** (151 mg, 86%) as red solid. The crude product was immediately used in next step.

Succinimidyl 4-[3,5-bis(trifluoromethyl)benzamido]benzoate (4): *N*-Hydroxysuccinimide (177 mg, 0.787 mmol), HOBt (120 mg,0.890 mmol), and

(A)

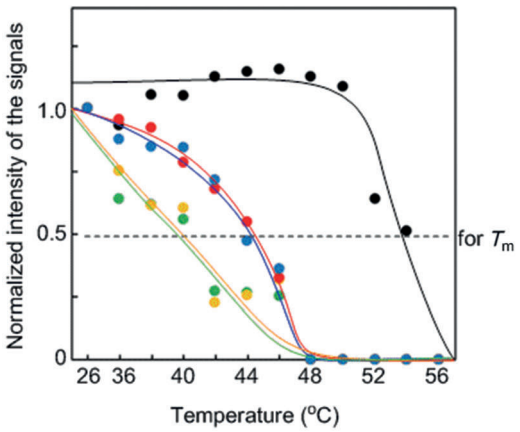

(B)

duplex	T_m(NMR)	T_m(UV)
ODN F2 / ODN T-Mis duplex	40 °C	41.6 °C
ODN F2 / ODN Comp duplex	54 °C	56.1 °C
ODN F2 / ODN G-Bul duplex	40 °C	41.6 °C
ODN F2 / ODN A-Bul duplex	45 °C	45.4 °C
ODN F2 / ODN G-Mis duplex	44 °C	44.8 °C

Figure 6. A) Change of the signal intensity attributed to each duplex and single-stranded ODN F2 (green: ODN F2/ODN T-Mis duplex; orange: ODN F2/ODN G-Bul duplex; blue: ODN F2/ODN G-Mis duplex; red: ODN F2/ODN A-Bul duplex; black: ODN F2/ODN Comp duplex) during heating from 26 to 56 °C. The concentration of each duplex at 26 °C was 50 μM. B) List of melting temperatures (T_m) of each duplex obtained from the signal intensity of the ^{19}F NMR spectrum (T_m (NMR)) or conventional UV measurement (T_m (UV)). For the NMR study, T_m was estimated as the temperature at which the signal intensity was reduced by half. For the UV study, T_m was estimated from the UV melting curve measured at 260 nm.

EDC (159 mg, 1.02 mmol) were added to a solution of **3** (135 mg, 0.359 mmol) in dry DMF (5.0 mL), and the resulting mixture was stirred for 22 h at 80 °C. After diluting with water, the reaction mixture was extracted with ethyl acetate. The organic layer was washed by brine, dried over anhydrous $MgSO_4$, filtered and then concentrated in vacuo. The crude product was purified by flash chromatography (SiO_2, 0.5 % methanol/chloroform) to give **4** (60 mg, 35 %) as red solid. M.p. 252–254 °C; ^{1}H NMR (300 MHz, $CDCl_3$): $\delta = 2.86$ (s, 4H), 7.72 (d, $J = 8.43$ Hz, 2H), 7.96 (d, $J = 8.76$ Hz, 2H), 8.02 (s, 1H), 8.34 (s, 2H), 8.61 ppm (s, 1H); ^{13}C NMR (75 MHz, $CDCl_3$): $\delta = 25.65$, 119.79, 127.76, 128.79, 130.89, 131.98, 132.21, 132.65, 136.39, 143.35, 161.04, 162.91, 169.70 ppm; FABMS (NBA): *m/z*: 475 $[M+H]^+$; HRMS calcd for $C_{20}H_{13}F_6N_2O_5$ 475.0729 $[M+H]^+$; found: 475.0727.

Preparation of ODN F1 (General procedure for the preparation of oligodeoxynucleotides possessing an F-unit): A solution of **1** (3.1 mg, 6.54 nmol) and sat. $NaHCO_3$ (20 μL) was added to a solution (total volume 170 μL) of the ODN N, and incubated at 37 °C for 8 h. The reaction mixture was purified by reversed HPLC. The purity and concentrationof given ODN F1 were determined by complete digestion by AP, P1, and phosphodiesterase I at 37 °C for 4 h. Identities of synthesized ODNs were confirmed by using ESI-TOF mass spectrometry (Thermoscientific exactive); ODN F1: *m/z* calcd: 1961.36 $[M-2H]^{2-}$; found: 1961.26; ODN F2: *m/z* calcd: 1345.15 $[M-3H]^{3-}$; found: 1346.56.

NMR spectroscopy: ^{19}F NMR spectra without ^{1}H-decoupling were measured at a frequency of 376.05 MHz and were referenced relative to internal CF_3COONa ($\delta = -76.5$ ppm). Experimental parameters were as follows: ^{19}F excitation pulse 8.00 μs, acquisition time 1.3 s, relaxation delay 5 s, number of scans ≈1000. The measurements of the ^{19}F NMR spectra of ODNs (50 μM) were conducted in the aqueous solution containing D_2O (20 %), phosphate Na (10 mM, pH 7.0), NaCl (100 mM) and CF_3COONa (100 μM).

Measurement of the melting temperature (T_m) by UV spectra: Melting temperatures (T_m) of the duplexes (2 μM, duplex concentration) were taken in a 10 mM Phosphate buffer (pH 7) containing 100 mM NaCl. Absorbance versus temperature profiles were measured at 260 nm with a heating rate of 1 °C min^{-1}. From these profiles, first derivatives were calculated to determine T_m values.

CD measurement: ODNs (2 μM) were dissolved in 10 mM phosphate buffer containing 100 mM NaCl. Spectra were recorded from 200 to 400 nm at 20 °C on a JASCO J-700 spectrophotometer, using 0.1 cm path length UV cell.

Acknowledgements

We thank Mr. Haruo Fujita and Ms. Eriko Kusaka (Graduate School of Synthetic Chemistry and Biological Chemistry, Kyoto Univeristy) for the measurement of ^{19}F–^{19}F differential NOE spectra.

[1] W. Saenger, *Principles of Nucleic Acid Structure*, Springer, New York **1984**.
[2] R. R. Sinden, *DNA Structure and Function*, Academic, New York **1994**.
[3] N. R. Cozzarelli, J. C. Wang, *DNA Topology and Its Biological Effects*, Cold Spring Harbor Laboratory Press, New York **1990**.
[4] E. C. Friedberg, G. C. Walker, W. Siede, *DNA Repair and Mutagenesis*, ASM, Washington **1995**.
[5] Y. Ionov, M. A. Peinado, S. Mlkhosyan, D. Shibata, M. Perucho, *Nature* **1993**, *363*, 558.
[6] G. Streisinger, Y. Okada, J. Emrich, J. Newton, A. Tsugita, E. Terzaghi, M. Inouye, *Cold Spring Harbor Symp. Quant. Biol.* **1966**, *31*, 77.
[7] G. V. Fazakerley, E. Quignard, A. Woisard, W. Guschlbauer, G. A. van der Marel, J. H. van Boom, M. Jones, M. Radman, *EMBO J.* **1986**, *5*, 3696.
[8] M. Radman, R. Wagner, *Curr. Top. Microbiol. Immunol.* **1984**, *108*, 23.
[9] A. L. Lu, S. Clark, P. Modrich, *Proc. Natl. Acad. Sci. USA* **1983**, *80*, 4639.
[10] L. Zídek, R. Štefl, V. Sklenář, *Curr. Opin. Struct. Biol.* **2001**, *11*, 275.
[11] B. Fürtig, C. Richter, J. Wöhnert, H. Schwalbe, *ChemBioChem* **2003**, *4*, 936.
[12] M. Mayer, T. L. James, *Methods Enzymol.* **2005**, *394*, 571.
[13] K. Tanabe, H. Harada, M. Narazaki, K. Tanaka, K. Inafuku, H. Komatsu, T. Ito, H. Yamada, Y. Chujo, T. Matsuda, M. Hiraoka, S. Nishimoto, *J. Am. Chem. Soc.* **2009**, *131*, 15982.
[14] J. T. Greig, in *Biological Magnetic Resonance* (Eds.: L. Berliner, J. Reuben), Plenum, New York, **1978**, p. 139.
[15] F. Rastinejad, C. Evilia, P. Lu, *Methods Enzymol.* **1995**, *261*, 560.
[16] N. B. Barhate, R. N. Barhate, P. Cekan, G. Drobny, S. T. Sigurdsson, *Org. Lett.* **2008**, *10*, 2745.

[17] K. Tanabe, M. Sugiura, S. Nishimoto, *Bioorg. Med. Chem.* **2010**, *18*, 6690.
[18] J. Riedl, R. Pohl, L. Rulíšek, M. Hocek, *J. Org. Chem.* **2012**, *77*, 1026.
[19] F. Wachowius, C. Höbartner, *ChemBioChem* **2010**, *11*, 469.
[20] B. Puffer, C. Kreutz, U. Rieder, M. O. Ebert, R. Konrat, R. Micura, *Nucleic Acids Res.* **2009**, *37*, 7728.
[21] A. Kiviniemi, P. Virta, *J. Am. Chem. Soc.* **2010**, *132*, 8560.
[22] D. Graber, H. Moroder, R. Micura, *J. Am. Chem. Soc.* **2008**, *130*, 17230.
[23] R. Moumné, M. Pasco, E. Prost, T. Lecourt, L. Micouin, C. Tisné, *J. Am. Chem. Soc.* **2010**, *132*, 13111.
[24] G. L. Olsen, E. A. Louie, G. P. Drobny, S. T. Sigurdsson, *Nucleic Acids Res.* **2003**, *31*, 5084.
[25] G. L. Olsen, T. E. Edwards, P. Deka, G. Varani, S. T. Sigurdsson, *Nucleic Acids Res.* **2005**, *33*, 3447.
[26] A. Kiviniemi, P. Virta, *Bioconjugate Chem.* **2011**, *22*, 1559.
[27] K. Fauster, C. Kreutz, R. Micura, *Angew. Chem.* **2012**, *124*, 13257; *Angew. Chem. Int. Ed.* **2012**, *51*, 13080.
[28] S. Jäger, G. Rasched, H. Kornreich-Leshem, M. Engeser, O. Thum, M. Famulok, *J. Am. Chem. Soc.* **2005**, *127*, 15071.
[29] K. Tanabe, H. Iida, K. Haruna, T. Kamei, A. Okamoto, S. Nishimoto, *J. Am. Chem. Soc.* **2006**, *128*, 692.
[30] H. Yamada, K. Tanabe, S. Nishimoto, *Bioorg. Med. Chem. Lett.* **2005**, *15*, 665.
[31] T. A. Early, J. Olmsted III, D. R. Kearns, A. G. Lezius, *Nucleic Acids Res.* **1978**, *5*, 1955.
[32] G. Varani, W. H. McClain, *EMBO Rep.* **2000**, *1*, 18.
[33] Other three duplexes possessing a C-bulge, T-bulge, and C–^{F2}U mismatch did not give discriminable signals, because the difference of their chemical shift was still small.
[34] E. G. Klauber, C. Kanta De, T. K. Shah, D. Seidel, *J. Am. Chem. Soc.* **2010**, *132*, 13624.

Received: July 16, 2013
Published online: September 23, 2013

